CROATICA CHEMICA ACTA CCACAA **73** (2) 541–567 (2000)

ISSN-0011-1643
CCA-2665

Original Scientific Paper

Forced Hydrolysis of Fe^{3+} Ions in $NH_4Fe(SO_4)_2$ Solutions Containing Urotropin

Svetozar Musić,[a,*] *Ankica Šarić,*[a] *Stanko Popović,*[b] *Kiyoshi Nomura,*[c] *and Tsuguo Sawada*[c]

[a] *Ruđer Bošković Institute, P. O. Box 180, HR-10002 Zagreb, Croatia*

[b] *Department of Physics, Faculty of Science, University of Zagreb, P. O. Box 331, HR-10002 Zagreb, Croatia*

[c] *School of Engineering, University of Tokyo, Hongo 7–3–1, Bunkyo-ku, Tokyo, 113 Japan*

Received July 1, 1999; revised September 15, 1999; accepted September 20, 1999

The effects of urotropin on the hydrolysis of Fe^{3+} ions in $NH_4Fe(SO_4)_2$ solutions at 90 °C were investigated using X-ray powder diffraction, ^{57}Fe Mössbauer spectroscopy, Fourier transform infrared spectroscopy, and transmission electron microscopy. Three concentrations of $NH_4Fe(SO_4)_2$ solutions, 0.03, 0.1 and 0.5 M, with varying initial amounts of urotropin were used in the experiments. Chemical and structural properties of the precipitates strongly depended on the concentrations of the reactants and the time of hydrolysis. In the early stages of Fe^{3+} hydrolysis, samples were dominantly amorphous. α-FeOOH, α-Fe_2O_3 and $NH_4Fe_3(OH)_6(SO_4)_2$ were crystalline phases detected in the precipitates; however, the specific phase composition of each precipitate depended on the experimental conditions. The possible formation of schwertmannite was not proven in the precipitates. It was suggested that the particles of amorphous fraction, as well as α-FeOOH particles, contained significant amounts of sulphates on external and internal surfaces due to the specific adsorption. Regularity in the phase composition of the precipitates, as a function of the experimental conditions, was found. Crystallite sizes of oxides were estimated on the basis of the broad-

* Author to whom correspondence should be addressed.

ening of diffraction lines. Mössbauer spectroscopy indicated superparamagnetic behavior of α-FeOOH particles. Formation of α-FeOOH particles of colloidal dimensions was proven by transmission electron microscopy.

Key words: hydrolysis of Fe^{3+}, $NH_4Fe(SO_4)_2$ solutions, urotropin

INTRODUCTION

Iron oxides (group name) have found important applications as pigments, catalysts, magnetic recording media, gas sensors, *etc*. They are also constituents of the soil and sediments. Mixtures of iron oxides, known as rust, are products of the corrosion of steel in water, air or soil. The phase composition of rust is strongly dependent on the conditions of steel corrosion.

Many factors may influence the formation of iron oxides from iron(II)- or iron(III)-salt solutions. Generally, the phase composition of a precipitate depends on the type of iron salts, pH, temperature, time of chemical reaction, *etc*. One of the most important factors, which strongly influences the formation of iron oxides, is the nature of the anion. In this introduction, we shall focus on selected works dedicated to the formation of iron oxides in the presence of the sulphate anion.

Musić *et al.*[1] used Mössbauer spectroscopy to monitor chemical changes in precipitates formed by forced hydrolysis of iron(III)-salt solutions. A mechanism for the formation of iron oxides, depending on the nature of the anion (Cl^-, NO_3^- or SO_4^{2-}) present in the solution, was proposed. Basic iron(III)-sulphates, obtained by forced hydrolysis of Fe^{3+} ions in the presence of sulphate anions, were subjected to thermal treatment.[2] Mössbauer spectra indicated the formation of $Fe_2O(SO_4)_2$ at 320 and 400 °C, and $Fe_2(SO_4)_3$ at 500 °C. α-Fe_2O_3 (hematite) was obtained as a single phase at 600 °C.

Sapieszko *et al.*[3] suggested that $FeOH^{2+}$ and $FeSO_4^+$ complexes play the dominant role in the formation of basic iron(III)-sulphates. With increasing temperature, the relative concentration of the $Fe(OH)_2^+$ complex increased, and at 80 °C this complex ion exceeded in content the primary hydroxy complex, $FeOH^{2+}$. Sulphate anions may influence the morphology of α-Fe_2O_3 particles formed by forced hydrolysis of the $FeCl_3$ solution. For example, Sugimoto *et al.*[4] observed the formation of ellipsoidal α-Fe_2O_3 particles in the presence of SO_4^{2-} or $H_2PO_4^-$ anions. The $H_2PO_4^-$ anion favoured single crystals of α-Fe_2O_3 particles, while in the presence of SO_4^{2-} anions, the internal substructure of the α-Fe_2O_3 particles was observed. Reeves and Mann[5] also investigated the influence of sulphate and other inorganic anions, as well as organic phosphorus anion, on the forced hydrolysis of the

$FeCl_3$ solution. The effect of SO_4^{2-} or $H_2PO_4^-$ anions on the morphology of α-Fe_2O_3 particles was explained by their specific adsorption on selected crystal planes. In the presence of the organic phosphorus anion, γ-FeOOH (lepidocrocite), α-Fe_2O_3 or β-FeOOH (akaganéite) were precipitated, and the formation of the specific oxide phase depended on the nature of the organic phosphorus anion.

Parida and Das[6] investigated the influence of sulphate anions on forced hydrolysis of a 0.1 M $Fe(NO_3)_3$ solution. In the absence of sulphate anions, the forced hydrolysis of the 0.1 M $Fe(NO_3)_3$ solution produced mixtures of α-FeOOH (goethite) and α-Fe_2O_3, whereas basic iron(III)-sulphates of varying composition were obtained from solutions with the concentration ratio $[SO_4^{2-}]/[Fe^{3+}] = 1$. For low concentrations of sulphate anions, the α-FeOOH particles showed a very narrow particle size distribution, spherical shape, microporous properties and a large surface area. Dutrizac[7] found that the initial rate of precipitation of $NH_4Fe_3(OH)_6(SO_4)_2$ or $NaFe_3(OH)_6(SO_4)_2$ (ammonium- or sodium jarosite) increased linearly with the addition of seed crystals. During the performance of this work, a minimum degree of agitation of the precipitation system for jarosite synthesis was determined, the pH range of jarosite precipitation was extended to lower pH values, and the temperature of jarosite precipitation was decreased. A porous jarosite, $KFe_3(OH)_6(SO_4)_2$, with a large specific area (150 $m^2\,g^{-1}$) was synthesized[8] by the chemical reaction between K_2SO_4 and $Fe_2(SO_4)_3$ under boiling conditions at pH 1.8 to 2.1. Musić *et al.*[9] investigated the phase composition and microstructural properties of solid phases formed by the hydrolysis of Fe^{3+} ions in $Fe_2(SO_4)_3$ solutions at 90 or 120 °C using X-ray powder diffraction, Mössbauer and FT-IR spectroscopies, and transmission electron microscopy. Experimental conditions were determined for the precipitation of α-FeOOH or $H_3OFe_3(OH)_6(SO_4)_2$ (hydronium jarosite) as a single phase. α-FeOOH particles showed superparamagnetic behaviour. $H_3OFe_3(OH)_6(SO_4)_2$ and basic sulphate, $Fe_4(OH)_{10}SO_4$, were obtained by the hydrolysis of Fe^{3+} ions as 0.1 M $Fe_2(SO_4)_3$ solution at 120 °C.

Basic iron(III)-sulphates can also be produced by bacterial activity. The oxidation of $FeSO_4$ solutions with *Thiobacillus ferrooxidans* bacteria cells produced crystalline jarosites, amorphous basic iron(III)-sulphates, or both.[10] The amorphous phase produced by bacterial oxidation of Fe^{2+} ions exhibited a distinctive fibrous microstructure. In the presence of excess sulphate and appropriate monovalent cations, crystalline jarosites were formed instead of amorphous basic iron(III)-sulphates. Sasaki *et al.*[11] investigated the role of the sulphur-oxidizing bacteria *Thiobacillus thiooxidans* in pyrite weathering to clarify the effects of this type of bacteria on the formation of secondary, iron containing minerals. *Thiobacillus thiooxidans* bacteria cells,

in the presence of the iron-oxidising *Thiobacillus ferrooxidans* bacteria cells, enhanced the dissolution of iron and sulphur ionic species from pyrite.

Understanding of acid mine drainage, the formation of secondary minerals and the adsorption/desorption of toxic heavy metals on secondary minerals is important for ecological reasons. It was found that goethite, lepidocrocite and jarosite precipitated from groundwater contaminated by mine waste leachate in Dalarna, Sweden.[12] Karathanasis and Thompson[13] analyzed precipitates formed at various stages of acid mine drainage treatment at Jones Branch wetland in McCreary County, Kentucky. Various minerals were detected, such as poorly crystalline ferrihydrite, lepidocrocite, akaganéite, basic iron(III)-sulphate and gypsum, and the phase composition of the precipitates depended on the location of wetland cells. Webster *et al.*[14] investigated pH-dependence of the adsorption of Cu^{2+}, Pb^{2+}, Zn^{2+} and Cd^{2+} onto the precipitates collected from acid drainage below a sulphide-bearing tailings dam at the former Tui Pb-Zn mine, near Te Aroha at Coromandel, New Zealand. Bigham *et al.*[15] characterized a poorly crystallized iron oxyhydroxysulphate formed by bacterial oxidation of Fe(II) in acid mine waters. The authors claimed that this compound differed from amorphous iron(III)-hydroxide or ferrihydrite. This compound (ideal formula $Fe_8O_8(OH)_6SO_4$) was later named schwertmannite.[16] Barham[17] prepared schwertmannite by the chemical precipitation method or using *Thiobacillus ferrooxidans* bacteria cells. Childs *et al.*[18] described the formation of schwertmannite in an entirely natural process, not influenced by mining operations, in Lake Matsuo-Goshikinuma (Towada-Hachimantai National Park, Honshu, Japan). It is interesting to note that the effect of schwertmannite precipitation was present from September to June each year due to favourable natural conditions, such as lake water circulation, a relatively high level of dissolved oxygen and an abundance of *Thiobacillus ferrooxidans* bacteria. Finally, it can be also mentioned that Bishop and Murad[19] discussed the possible presence of schwertmannite on planet Mars. On the basis of a critical evaluation of geochemical, thermodynamic and spectroscopic data, it was concluded that during the history of Mars all the conditions necessary for the formation of mineral schwertmannite on that planet existed.

In the present work, we focus on the precipitation process from $NH_4Fe(SO_4)_2$ solutions with varying concentrations of urotropin (hexamethylenetetramine) added at the beginning of the precipitation process. Urotropin served as a generator of OH^- ions. In acidic pH medium at elevated temperature, urotropin undergoes hydrolysis in accord with formal chemical reactions:

$$(CH_2)_6N_4 + 6H_2O \rightarrow 4NH_3 + 6HCHO \quad (1)$$

and

$$NH_3 + H_2O \rightarrow NH_4^+ + OH^-. \quad (2)$$

In the present work, the concentration ranges of the chemical reactants were extended in relation to many previous works in this field in order to obtain better information about the overall precipitation process. Addition of urotropin also made it possible to extend the pH region of the Fe^{3+} hydrolysis, as well as to eliminate the problems that can occur with an abrupt addition of NaOH or NH_4OH solution to the precipitation system. Even in the case of controlled addition of NaOH or NH_4OH solution, it is impossible to have conditions like those with urotropin, which occur in the latter case at the molecular level. Finally, the time of aging of the precipitation systems was long enough to observe the tendencies in the phase transformations of the precipitates.

EXPERIMENTAL

$NH_4Fe(SO_4)_2 \cdot 12H_2O$ and urotropin, both of analytical grade purity, and doubly distilled water were used for the preparation of samples. For the preparation of $NH_4Fe(SO_4)_2$ solutions, only fresh $NH_4Fe(SO_4)_2 \cdot 12H_2O$ salt, as obtained from the supplier, was used. If an old $NH_4Fe(SO_4)_2 \cdot 12H_2O$ (stored for a long time) is used, there is a problem of its complete dissolution in water due to the previous hydrolysis of Fe^{3+} ions in the solid state. Chemical composition of the solutions and other experimental data for the preparation of samples are given in Table I. The total volume of each precipitation system was 200 mL. The aging of the precipitation systems was performed in glass autoclaves at 90 °C. After a proper aging time, solid hydrolytical products were separated from the mother liquor using an ultraspeed centrifuge, Sorvall RC2-B (operational range up to 20 000 r.p.m.). Solid hydrolytical products were subsequently washed with doubly distilled water and then dried.

pH measurements were performed using a pH meter, model PHM–26, and a combined glass-calomel electrode (operational range up to pH 14), both manufactured by Radiometer.

X-ray powder diffraction measurements were performed using the Philips diffractometer, (model MPD 1880, Cu$K\alpha$ radiation, graphite monochromator, proportional counter).

The FT-IR spectra were recorded using a Perkin-Elmer spectrometer, model 2000. The IRDM (Infrared Data Manager) program, obtained by Perkin-Elmer, was used to process the recorded spectra. The specimens were pressed into a KBr matrix.

^{57}Fe Mössbauer spectra were recorded using standard equipment and a $^{57}Co/Rh$ source. Mathematical deconvolutions of the recorded spectra were performed using a standard procedure.

Selected samples were characterized with electron microscopy (Opton, model EM–10). Before the TEM observation, the powders were dispersed in doubly distilled water using an ultrasonic bath and then a drop of the dispersion was put on a copper grid, previously covered with a polymer film.

TABLE I

Experimental conditions for the preparation of samples at 90 °C

Sample	$[NH_4Fe(SO_4)_2]$ / mol dm^{-3}	[Urotropin] / mol dm^{-3}	Time of aging	pH (final)
S1	0.03		6 h	1.78
S2	0.03		1 d	1.92
S3	0.03		3 d	1.86
S4	0.03		7 d	1.82
S5	0.03		21 d	1.34
S6	0.03	0.03	6 h	4.85
S7	0.03	0.03	1 d	4.81
S8	0.03	0.03	3 d	4.75
S9	0.03	0.03	7 d	4.73
S10	0.03	0.03	21 d	4.77
S11	0.03	0.1	6 h	5.58
S12	0.03	0.1	1 d	6.28
S13	0.03	0.1	3 d	6.35
S14	0.03	0.1	7 d	6.56
S15	0.03	0.1	21 d	7.46
S16	0.03	0.25	6 h	5.90
S17	0.03	0.25	1 d	6.73
S18	0.03	0.25	3 d	6.97
S19	0.03	0.25	7 d	7.28
S20	0.03	0.25	21 d	8.39
S21	0.1		6 h	2.15
S22	0.1		1 d	1.85
S23	0.1		3 d	1.70
S24	0.1		7 d	1.62
S25	0.1		21 d	1.17
S26	0.1	0.025	6 h	2.11
S27	0.1	0.025	1 d	1.75
S28	0.1	0.025	3 d	1.70
S29	0.1	0.025	7 d	1.65
S30	0.1	0.025	21 d	1.21
S31	0.1	0.1	6 h	3.42
S32	0.1	0.1	1 d	3.40
S33	0.1	0.1	3 d	4.00
S34	0.1	0.1	7 d	6.34
S35	0.1	0.1	21 d	6.96
S36	0.1	0.25	6 h	5.29
S37	0.1	0.25	1 d	5.62
S38	0.1	0.25	3 d	5.77
S39	0.1	0.25	7 d	
S40	0.1	0.25	21 d	8.22

TABLE I (continued)

Sample	$[NH_4Fe(SO_4)_2]$ / mol dm^{-3}	[Urotropin] / mol dm^{-3}	Time of aging	pH (final)
S41	0.5		1 d	1.50
S42	0.5		7 d	0.72
S43	0.5		21 d	0.74
S44	0.5	0.025	1 d	1.55
S45	0.5	0.025	7 d	0.80
S46	0.5	0.025	21 d	0.77
S47	0.5	0.1	6 h	1.90
S48	0.5	0.1	1 d	1.30
S49	0.5	0.1	7 d	0.82
S50	0.5	0.1	21 d	0.82
S51	0.5	0.25	6 h	1.84
S52	0.5	0.25	1 d	1.62
S53	0.5	0.25	7 d	1.25
S54	0.5	0.25	21 d	1.30
S55	0.5	0.5	6 h	2.17
S56	0.5	0.5	1 d	3.21
S57	0.5	0.5	7 d	7.75
S58	0.5	0.5	21 d	8.54
S59	0.5	1	6 h	3.37
S60	0.5	1	1 d	4.82
S61	0.5	1	7 d	7.78
S62	0.5	1	21 d	8.87

Key: h = hour; d = day

RESULTS AND DISCUSSION

X-ray Powder Diffraction

The phase composition of selected samples, as determined by X-ray powder diffraction, is given in Table II. Crystalline phases were identified according to the data contained in the ICDD Powder Diffraction File:[20] $NH_4Fe_3(OH)_6(SO_4)_2$, card no. 26–1024; α-Fe_2O_3, cards no. 13–534, or 33–664 and α-FeOOH, cards no. 17–536, or 29–713. Samples S1, S6, S11 and S16, obtained from a 0.03 M $NH_4Fe(SO_4)_2$ solution after 6 hours at 90 °C, were amorphous, as shown by XRD. In sample S6, very broad bands at the positions of the most prominent diffraction lines of α-FeOOH, having very small crystallites, were additionally observed. XRD analysis of samples S17 to S20 showed a tendency to crystallization of α-FeOOH and α-Fe_2O_3 with a

TABLE II

Phase composition of selected samples as determined by X-ray powder diffraction

Sample	Phase composition	Remark		
S1	AM			
S6	AM + G^a			
S11	AM			
S16	AM			
S17	AM + G** + H**			
S18	H + G	BDL	|	an increase of the
S19	H + G	BDL	|	sharpness of
S20	H + G	BDL	↓	diffraction lines
S21	AJ + AM	SDL	|	a small increase
S22	AJ	SDL	|	of the sharpness of
S23	AJ	SDL	|	diffraction
S24	AJ	SDL	↓	lines
S25	AJ + G^a	LBDL		
S26	AM + G^a			
S31	AM + G^a			
S36	AM + G^a			
S41	AJ	SDL	|	a small increase
S42	AJ	SDL	|	of the sharpness of
S43	AJ	SDL	↓	diffraction lines
S47	AJ + AM	LBDL		
S55	AM			
S59	G	VBDL		

Key: AM = amorphous; G = α-FeOOH (goethite); G^a = very broad bands at the positions of the most prominent goethite diffraction lines (very small crystallite size); H = α-Fe_2O_3 (hematite); AJ = $NH_4Fe_3(OH)_6(SO_4)_2$ (ammonium jarosite); SDL = sharp diffraction lines; LBDL = little broadened diffraction lines (crystallite size up to 100 nm); BDL = broadened diffraction lines (crystallite size of several tens of nm); VBDL = very broadened diffraction lines (crystallite size of the order of 10 nm); ** very small amount

prolonged time of hydrolysis. In the samples isolated between 3 and 21 days of hydrolysis, α-Fe_2O_3 was dominant in relation to α-FeOOH, both having broadened diffraction lines, indicating a crystallite size of several tens of nm.

In samples S21 to S25, obtained from a 0.1 M $NH_4Fe(SO_4)_2$ solution, with a hydrolysis time between 6 hours and 21 days, XRD showed the presence of $NH_4Fe_3(OH)_6(SO_4)_2$ as the major phase. A small increase in the sharpness of the diffraction lines with a prolonged time of hydrolysis was

observed. An amorphous fraction in sample S21 and α-FeOOH of very small crystallite size in sample S25 were additionally detected. XRD analysis of samples S26, S31 and S36, obtained after 6 hours of hydrolysis at 90 °C from 0.1 M $NH_4Fe(SO_4)_2$ solution with varying concentration of urotropin (0.025 to 0.25 M), showed the presence of an amorphous fraction and α-FeOOH of very small crystallite size.

With an increase of the concentration of $NH_4Fe(SO_4)_2$ up to 0.5 M, the conditions for formation of $NH_4Fe_3(OH)_6(SO_4)_2$, as a single phase, were created (samples S41, S42 and S43). For a short period of hydrolysis (6 hours) the phase composition strongly depended on the concentration of urotropin (samples S47, S55 and S59).

In order to ascertain by XRD the possible presence of schwertmannite in our samples, especially in those precipitated in short times of $NH_4Fe(SO_4)_2$ hydrolysis, we compared literature data[21] on the XRD peak positions for jarosite, schwertmannite and goethite with the XRD patterns of our samples. However, this comparison did not give any evidence of the presence of schwertmannite in our samples.

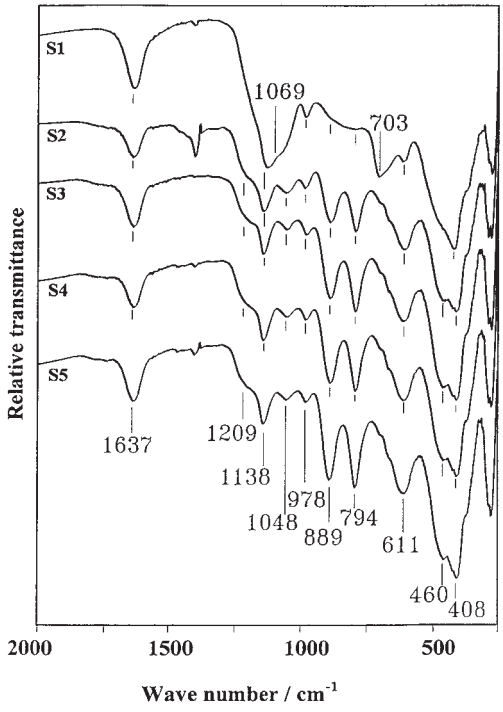

Figure 1. Fourier transform IR spectra of samples S1 to S5, recorded at room temperature.

FT-IR Spectroscopy

All samples were characterized by FT-IR spectroscopy, and the typical results of these measurements are presented in Figures 1, 2, 3 and 4. The FT-IR spectrum of sample S1 (Figure 1) shows a very strong band at 1138 cm^{-1} with a shoulder at 1069 cm^{-1} and a band at 978 cm^{-1} due to the presence of the sulphate group. The shoulder at 1209 cm^{-1} is clearly visible for the series of samples S2 to S5, as shown in the same figure. The FT-IR spectrum of sample S1 also shows a very broad band in the region ~790 to ~890 cm^{-1}, as well as bands at 703, 611 and 408 cm^{-1}. In the region of the very broad band at ~790 cm^{-1} to ~890 cm^{-1} for sample S1, other samples in the series, S2 to S5, show IR bands at 889 and 794 cm^{-1}, which can be assigned to Fe-O-OH bending vibrations in α-FeOOH. Verdonck *et al.*[22] used the method of normal coordinate analysis (NCA) to interpret the IR spectrum of α-FeOOH. Also, the IR spectrum of deuterated α-FeOOD was recorded. The IR bands at 630, 495 and 270 cm^{-1} were rather insensitive to deuteration and, for this reason, these bands were ascribed to Fe-O stretching vibra-

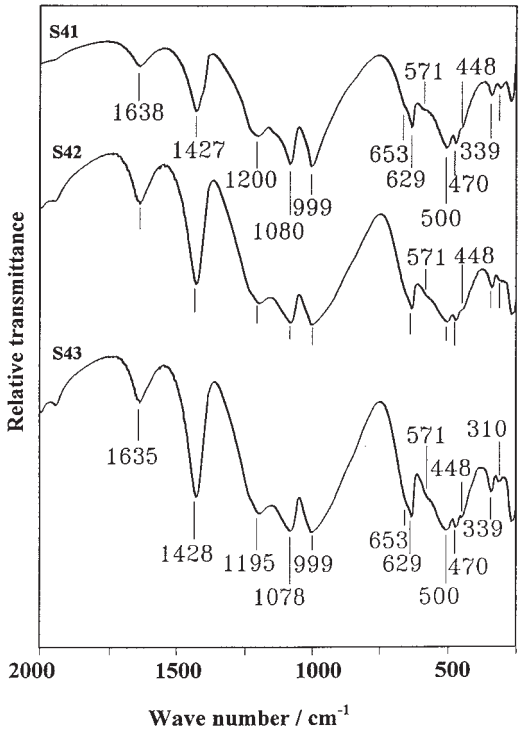

Figure 2. Fourier transform IR spectra of samples S41, S42 and S43 in the region of lower wave numbers. The spectra were recorded at room temperature.

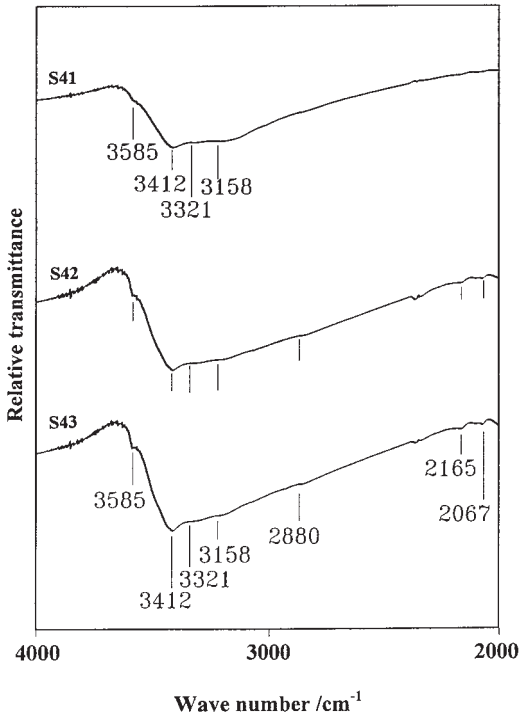

Figure 3. Fourier transform IR spectra of samples S41, S42 and S43 in the region of high wave numbers. The spectra were recorded at room temperature.

tions.[22] Cambier[23] assigned bands at 892 and 795 cm^{-1} to the OH bending vibrations in α-FeOOH. Interpretation of IR bands below 650 cm^{-1} was in accord with the interpretation of Verdonck *et al.*[22] Morterra *et al.*[24] used IR spectroscopy to investigate dehydration of commercial α-FeOOH samples and their phase transformation to α-Fe_2O_3.

The IR band at 1637 cm^{-1}, recorded for samples S1 to S5, is usually interpreted as the H_2O bending mode. On the basis of the FT-IR spectrum of sample S1, it can be concluded that sample S1 is dominantly amorphous, containing poorly ordered α-FeOOH. Significant amounts of sulphate ions are present on external and internal surfaces. It can be mentioned here that IR spectra similar to the spectrum of sample S1 were published in the literature for the schwertmannite formed by bacterial oxidation of Fe^{2+} in acid mine waters[15,25] and schwertmannite obtained in chemical laboratory.[14,17] A certain similarity between the IR spectra of schwertmannite and β-FeOOH were observed.[15] The very strong band corresponding to ν_{Fe-O} vibrations in schwertmannite varied in the range from 410 to 460 cm^{-1}.

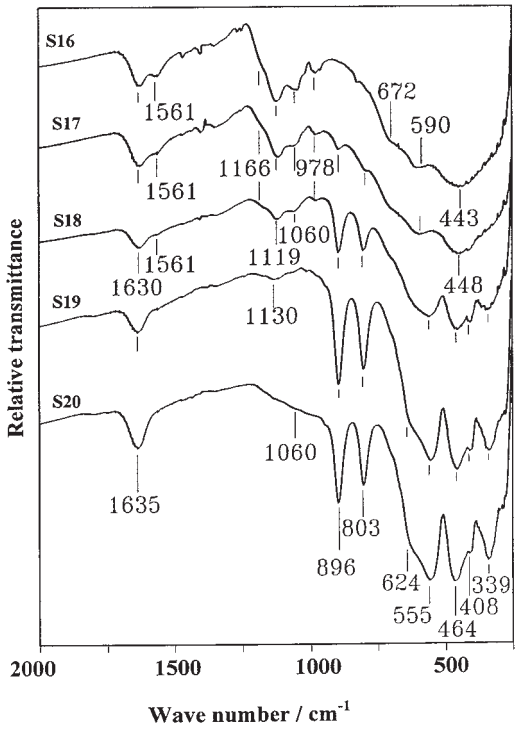

Figure 4. Fourier transform IR spectra of samples S16 to S20, recorded at room temperature.

Figures 2 and 3 show FT-IR spectra of samples S41, S42 and S43. These FT-IR spectra can be ascribed to $NH_4Fe_3(OH)_6(SO_4)_2$ as a single phase. The literature IR data for $NH_4Fe_3(OH)_6(SO_4)_2$ and some compounds containing NH_4^+ and/or SO_4^{2-} ions are given in Table III. This table also contains assignations of the presented[26–28] IR bands and, for this reason, the assignations of the IR bands shown in Figures 2 and 3 will not be additionally discussed in the text.

Figure 4 shows the FT-IR spectra of the samples in series S16 to S20. The FT-IR spectrum of sample S16 shows a very strong and broad band at 443 cm^{-1} with shoulders at 590 and 672 cm^{-1} and also bands typical of the sulphate group. This spectrum can be ascribed to an amorphous phase containing a significant amount of sulphate anions. With a prolonged time of heating of this precipitation system there is an increase of pH up to 8.39 after 21 days. The relative intensity of the IR bands corresponding to sulphate anions gradually decreases with the increase of pH and this is in accord with the adsorption of other oxyanions on iron(III)-hydrous oxide[29] and op-

TABLE III

Infrared data for $NH_4Fe_3(OH)_6(SO_4)_2$ and some compounds containing NH_4^+ and/or SO_4^{2-} ions

$NH_4Fe_3(OH)_6(SO_4)_2$ Assign.[26]		$H_3OFe_3(OH)_6(SO_4)_2$ Assign.[27]		$Fe(OH)SO_4$ Assign.[27]		$(NH_4)_3H(SO_4)_2$ Assign.[28]	
3420	ν_{OH}	3450	$\nu(OH^-)$	3450	$\nu(OH^-)$		
3340 3220 1655 1428	$\nu(NH_4^+)$					3223 3043 2855	$\nu_1, \nu_3 NH_4^+$
1195	ν_3(S-O)	1160 1095 1050	$\nu_3 SO_4^{2-}$ bidentate	1165 1100 1055	$\nu_3 SO_4^{2-}$ bidentate	1733 1680	$\nu_2 NH_4^+$
1078	ν_3(S-O)	1130	$\nu_3 SO_4^{2-}$ ionic	1125	$\nu_3 SO_4^{2-}$ ionic	1414	$\nu_4 NH_4^+$
1006	δ_{OH}	1015	δ(Fe-OH)	1005	δ(Fe-OH)	1180	δ_{OH}
1000	ν_1(S-O)	1000	$\nu_1 SO_4^{2-}$ bidentate	968	$\nu_1 SO_4^{2-}$ bidentate	1125	$\nu_3 SO_4^{2-}$
655	ν_4(S-O)	642 630 580	$\nu_4 SO_4^{2-}$ bidentate	647 634 582	$\nu_4 SO_4^{2-}$ bidentate	1080	$\nu_1 SO_4^{2-}$
630	ν_4(S-O)					960	$\nu_1 HSO_4^-$
560	γ_{OH}	612	$\nu_4 SO_4^{2-}$ ionic	616	$\nu_4 SO_4^{2-}$ ionic	910	γ_{OH}
505 472	O-Fe	525	ν(Fe-OH)	520	ν(Fe-OH)	597 570	$\nu_4 SO_4^{2-}$
450	ν_2(S-O)	460	$\nu_2 SO_4^{2-}$ bidentate	462	$\nu_2 SO_4^{2-}$ bidentate	444	$\nu_2 SO_4^{2-}$
345 320 265 233 204	O-Fe	360 335 295	ν(Fe-OSO_3)	380 327 280 252	ν(Fe-OSO_3)	216	νOH···O
158 110							

posite to the adsorption of metal cations on the same adsorbent.[30] FT-IR spectra of the samples in series S17 to S20 also show crystallization of α-FeOOH (bands at 803 and 896 cm^{-1}) and α-Fe_2O_3 (bands at 555 and 464 cm^{-1}). Iglesias and Serna[31] reported IR bands for α-Fe_2O_3 spheres at 575, 485, 385 and 360 cm^{-1}, and for α-Fe_2O_3 laths at 650, 525, 440 and 300 cm^{-1}. The crystallinity of α-Fe_2O_3 also influenced the corresponding IR spectrum.[32]

TABLE IV

FT-IR spectroscopic analysis of the samples prepared at 90 °C

Time of Heating	$[NH_4Fe(SO_4)_2]$ = 0.03 mol dm^{-3}			
	[Urotropin] / mol dm^{-3}			
	0	0.03	0.1	0.25
6 h	AM, G**	AM, G**	AM, G**	AM
24 h	G	H, G	AM, G, H***	AM, G**
72 h	G	H, G	G, H	H, G
7 d	G	H, G	H, G	H, G
21 d	G	H, G*	H, G	H, G
Time of Heating	$[NH_4Fe(SO_4)_2]$ = 0.1 mol dm^{-3}			
	[Urotropin] / mol dm^{-3}			
	0	0.025	0.1	0.25
6 h	AJ, (AM)	G, (AM)	G, (AM)	AM, G*
24 h	AJ	G	G	H, G
72 h	AJ, G*	G	G	G, H
7 d	AJ, G**	G	G	G, H
21 d	AJ, G*	G	G	G, H

Time of Heating	$[NH_4Fe(SO_4)_2]$ = 0.5 mol dm^{-3}					
	[Urotropin] / mol dm^{-3}					
	0	0.025	0.1	0.25	0.5	1
6 h			AJ, (AM)	AM***	AM***	G
24 h	AJ	AJ	AJ	G, AJ	G	G
7 d	AJ	AJ	AJ	AJ, G	G	G
21 d	AJ	AJ	AJ	AJ, G	G	G

Key: h = hour; d = day; AM = amorphous; G = α-FeOOH (goethite); H = α-Fe_2O_3 (hematite); AJ = $NH_4Fe_3(OH)_6(SO_4)_2$ (ammonium jarosite); *small amount; **very small amount; ***possible presence

Table IV shows the phase composition of samples in dependence on the concentration of chemical reactants and time of hydrolysis (aging) at 90 °C, as determined by FT-IR spectroscopy. A regularity in the formation of solid phases by forced hydrolysis of $NH_4Fe(SO_4)_2$ solutions and the effect of urotropin is clearly visible. α-FeOOH was formed as a single phase by the forced hydrolysis of 0.03 M $NH_4Fe(SO_4)_2$, $NH_4Fe_3(OH)_6(SO_4)_2$ and its mixtures with α-FeOOH were formed in 0.1 M $NH_4Fe(SO_4)_2$ solution, while the hy-

drolysis of 0.5 M $NH_4Fe(SO_4)_2$ solution yielded $NH_4Fe_3(OH)_6(SO_4)_2$ as a single phase. With the initial addition of urotropin in the concentration range from 0.03 to 0.25 M, after 6 hours of hydrolysis of 0.03 M $NH_4Fe(SO_4)_2$ solutions at 90 °C, an amorphous-like fraction and a very small amount of α-FeOOH were formed. In some cases, the FT-IR spectrum was similar to that of schwertmannite; however, on the basis of the FT-IR spectrum alone it would be difficult to identify it in the precipitates. In the previous section, it was shown that XRD did not give any evidence of the presence of schwertmannite in the investigated samples. In other samples, for higher initial concentrations of urotropin and a longer time of hydrolysis, mixtures of α-Fe_2O_3 and α-FeOOH were observed. Mixtures of α-FeOOH and α-Fe_2O_3 were obtained in solutions initially containing 0.1 M $NH_4Fe(SO_4)_2$ and 0.25 M urotropin. The formation of α-Fe_2O_3 was not detected by FT-IR spectroscopy in any sample obtained from 0.5 M $NH_4Fe(SO_4)_2$ with initial concentrations of urotropin varying from 0.025 to 1 M. $NH_4Fe_3(OH)_6(SO_4)_2$, α-FeOOH or mixtures of these two phases were formed in these precipitation systems.

^{57}Fe Mössbauer Spectroscopy

The Mössbauer spectroscopic results obtained for the selected samples are summarized in Figures 5 to 10 and in Table V.

RT Mössbauer spectra of solid products precipitated by the hydrolysis of Fe^{3+} ions in 0.03 M $NH_4Fe(SO_4)_2$ solution at 90 °C are shown in Figures 5 and 6, and numerical values of the hyperfine interactions are given in Table V. The spectrum of sample S1 (6 hours of hydrolysis) is characterized

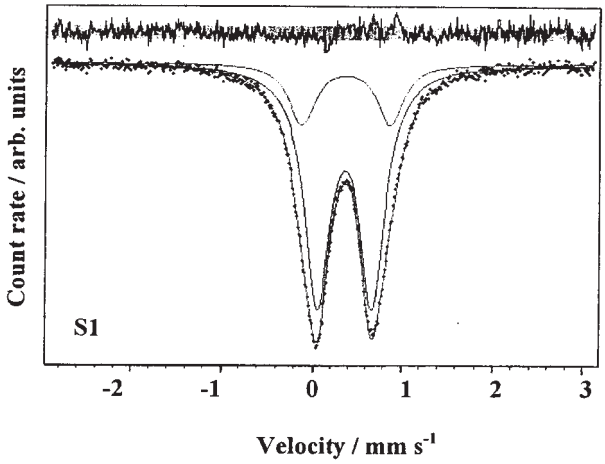

Figure 5. ^{57}Fe Mössbauer spectrum of sample S1, recorded at room temperature.

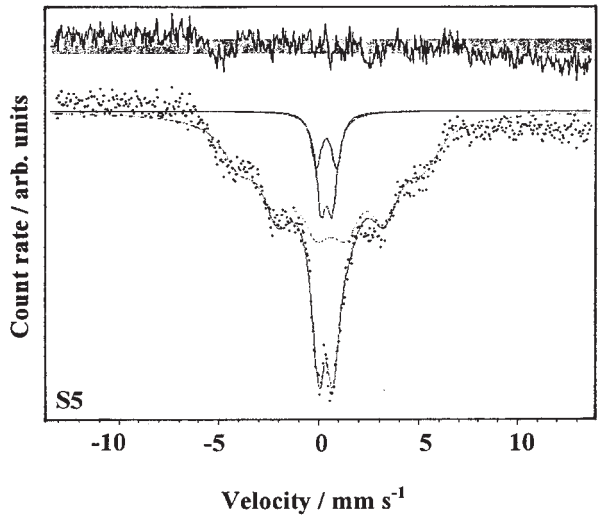

Figure 6. ^{57}Fe Mössbauer spectrum of sample S5, recorded at room temperature.

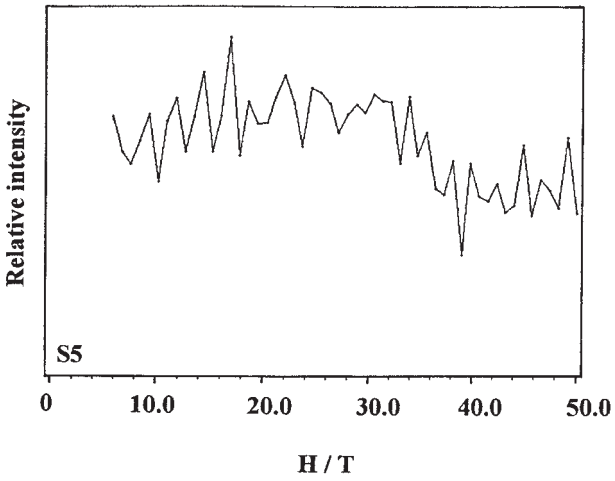

Figure 7. Distribution of hyperfine fields for sample S5.

by a central quadrupole doublet, and this spectrum can be actually considered as the distribution of quadrupole doublets. In the present work, it is fitted for two average doublets, as shown in Figure 5. A similar spectrum was recorded for sample S2, isolated after 1 day of hydrolysis. These Mössbauer spectra are in accordance with the results of XRD and FT-IR spectroscopic measurements performed with the same samples. As already docu-

mented in Tables II and IV, samples S1 and S2 consisted of an amorphous fraction and very fine (superparamagnetic) α-FeOOH particles. Figure 6 shows the RT Mössbauer spectrum of sample S5. Sample S5, precipitated

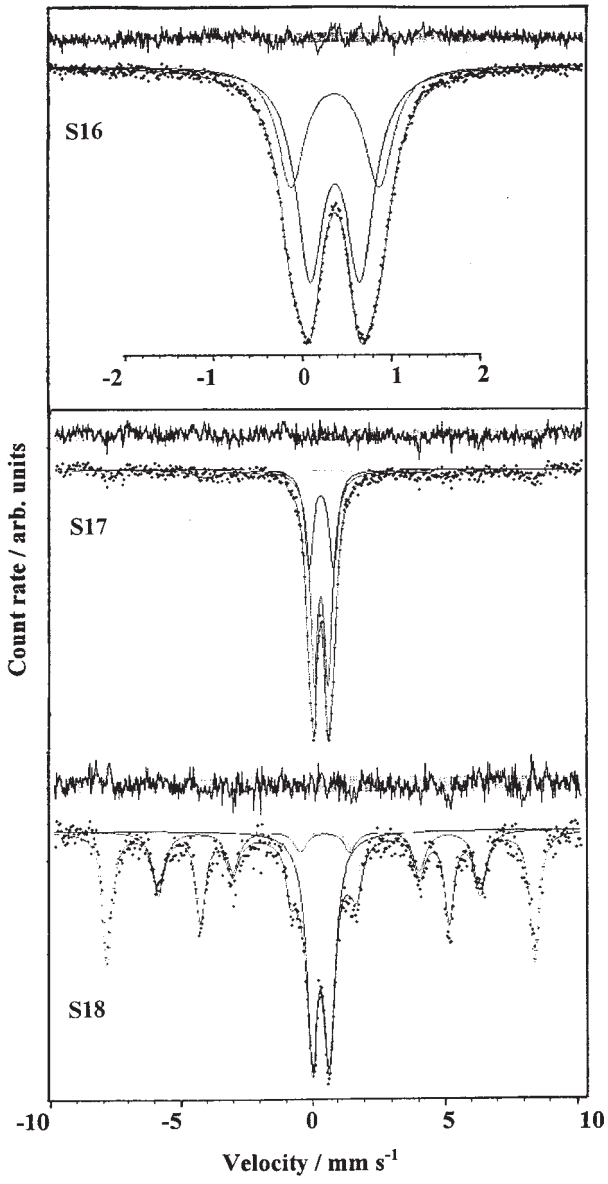

Figure 8. ^{57}Fe Mössbauer spectra of samples S16, S17 and S18, recorded at room temperature.

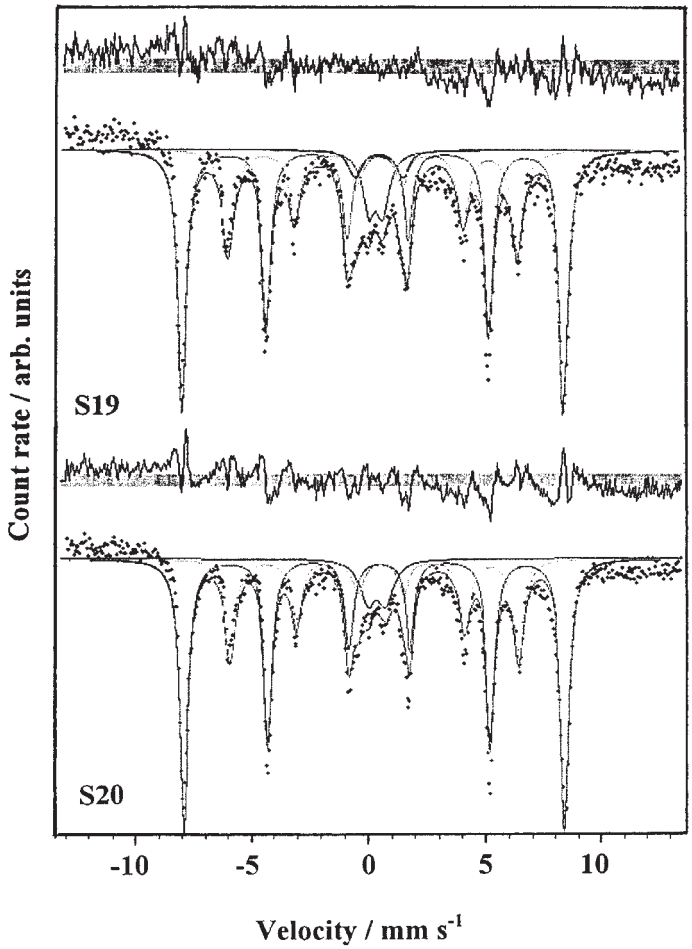

Figure 9. ^{57}Fe Mössbauer spectra of samples S19 and S20, recorded at room temperature.

for 21 days by the hydrolysis of 0.03 M $NH_4Fe(SO_4)_2$ solution at 90 °C, showed a superposition of the central quadrupole doublet and the collapsing sextet. The distribution of hyperfine fields was calculated and is shown in Figure 7. The central part of the spectrum was fitted for two average quadrupole doublets, like for samples S1 and S2. Taking into account the results of FT-IR spectroscopic analysis, it can be concluded that sample S5 consisted of α-FeOOH particles of different sizes. Poor crystallinity of a certain fraction of α-FeOOH particles and the possible presence of an amorphous fraction can not be excluded.

RT Mössbauer spectra of the solid products obtained by the hydrolysis at 90 °C of a 0.03 M $NH_4Fe(SO_4)_2$ solution containing initially 0.25 M urotropin are shown in Figures 8 and 9. The spectrum of sample S16 is characterized by a central quadrupole doublet representing the distribution of doublets, and in the present work it is fitted for two average doublets. XRD and FT-IR analysis of this sample showed only the presence of an amorphous fraction. The spectrum of sample S17 showed additionally a hyperfine magnetic splitting of very small intensity and this result is also in accordance with XRD and FT-IR spectroscopic measurements. With a further increase of hydrolysis time, the relative intensity of the central quadrupole doublet decreased and, consequently, the relative intensity of magnetic splitting increased (samples S18, S19 and S20). For sample S20, the outer

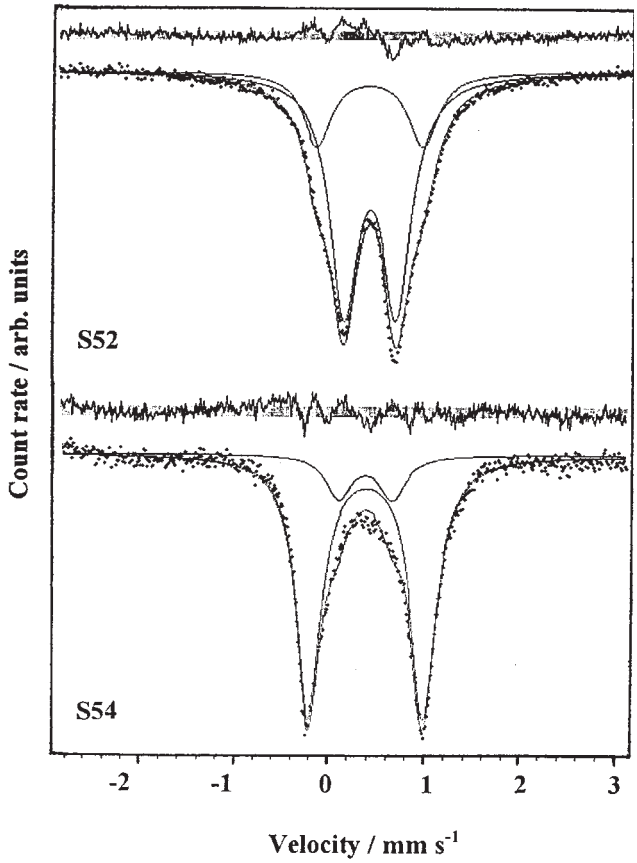

Figure 10. ^{57}Fe Mössbauer spectra of samples S52 and S54, recorded at room temperature.

sextet was characterized by H = 508 kOe corresponding to α-Fe_2O_3, whereas the inner sextet showed H = 383 kOe corresponding to α-FeOOH.

RT Mössbauer spectra of samples S52 and S54 are shown in Figure 10. These samples were obtained by hydrolysis, at 90 °C, of a 0.5 M $NH_4Fe(SO_4)_2$ solution containing 0.25 M urotropin at the beginning of the precipitation process. The spectrum of sample S52 (1 day of hydrolysis) showed an asymmetric quadrupole doublet, which was resolved into two doublets (Q_1 = 0.53 mm s^{-1} and Q_2 = 1.08 mm s^{-1}). For a prolonged time of hydrolysis, up to 21 days, the relative intensity of the inner doublet significantly decreased with a corresponding increase of the intensity of the outer doublet. For sample S54, the quadrupole splittings were measured, Q_1 = 0.56 mm s^{-1} and Q_2 = 1.19 mm s^{-1}. Taking into account the results of FT-IR spectroscopy, the inner doublet can be ascribed to a superparamagnetic α-FeOOH, whereas the outer doublet is due to the presence of $NH_4Fe_3(OH)_6(SO_4)_2$.

TABLE V

^{57}Fe Mössbauer parameters of selected samples

Sample	Spectral lines	δ / mm s^{-1}	Δ / mm s^{-1}	Γ / mm s^{-1}	A / %
S1	Q_1	0.36	0.62	0.35	79.2
	Q_2	0.37	1.00	0.35	20.8
S2	Q_1	0.36	0.53	0.37	83.6
	Q_2	0.35	1.11	0.37	16.4
S5	Q_1	0.39	0.56	0.55	65.8
	Q_2	0.44	1.28	0.55	34.2
S16	Q_1	0.34	0.57	0.37	62.5
	Q_2	0.34	0.99	0.37	37.5
S17	Q_1	0.34	0.56	0.39	67.8
	Q_2	0.33	0.97	0.39	32.2
S52	Q_1	0.36	0.53	0.35	75.6
	Q_2	0.35	1.08	0.35	24.4
S54	Q_1	0.37	0.56	0.32	14.3
	Q_2	0.39	1.19	0.32	85.7

Key: δ = isomer shift given relative to α-Fe; Δ = quadrupole splitting of doublet Q; Γ = line-width; A = area under the peaks

Error in δ and Δ estimated to ±0.01 mm s^{-1}

Transmission Electron Microscopy

Transmission electron microphotographs of the selected samples are shown in Figures 11 to 15. Figure 11 shows electron microphotographs of α-FeOOH particles formed by aging of 0.03 M $NH_4Fe(SO_4)_2$ solution at 90 °C for 7 and 21 days, respectively (samples S4 and S5). A detailed observation showed irregular ends of these particles, thus indicating their substructure, *i.e.*; they can be considered as bundles of α-FeOOH needles. Figures 12 and 13 show electron microphotographs of the precipitates formed by forced

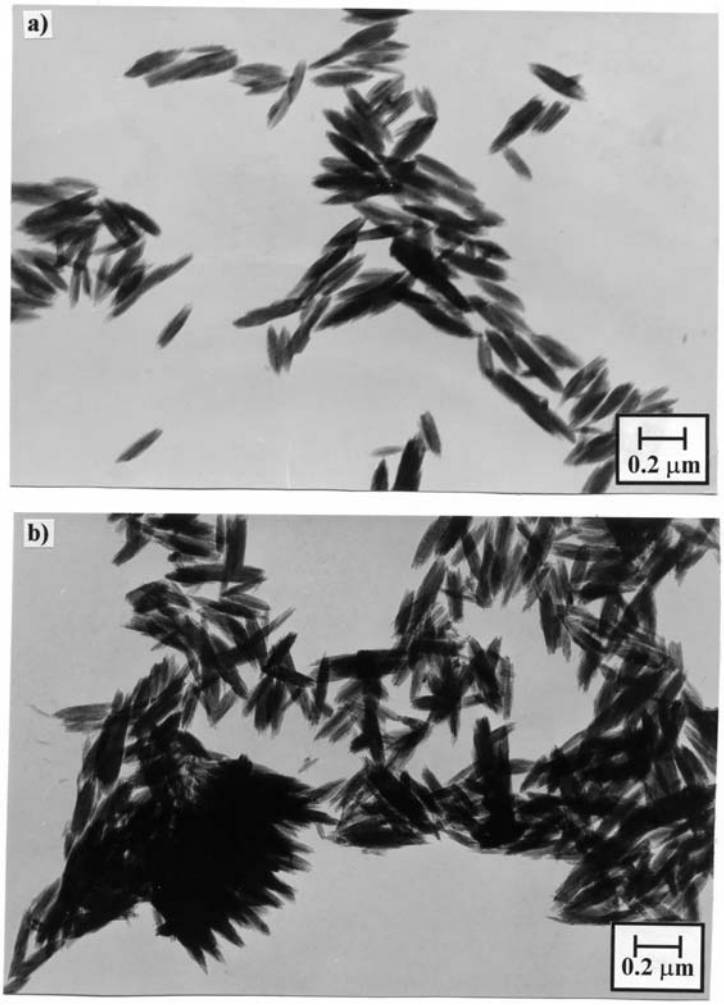

Figure 11. Transmisssion electron microphotographs of samples (a) S4 and (b) S5.

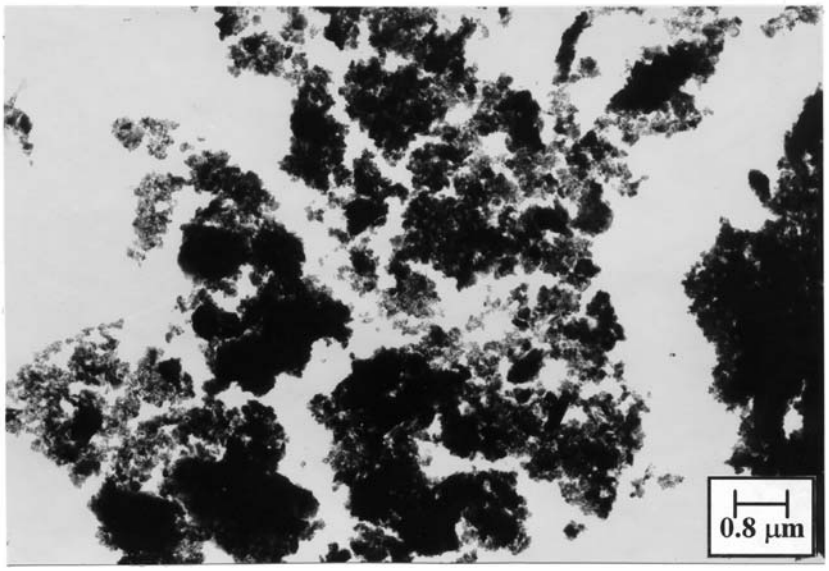

Figure 12. Transmisssion electron microphotograph of sample S17.

hydrolysis of the solution 0.03 M $NH_4Fe(SO_4)_2$ + 0.25 M urotropin. After one day of aging of the precipitation system at 90 °C, the aggregates of small particles were visible (sample S17). Sample S17 contained predominantly an amorphous fraction and very small amounts of α-FeOOH and α-Fe_2O_3, as found with XRD. Between 7 and 21 days of aging of the above-mentioned precipitation system at 90 °C, the electron microphotographs of the corresponding precipitates (samples S19 and S20) showed that α-Fe_2O_3 polyhedra were dominant. α-FeOOH needles were also visible. Electron microphotographs of samples S25 and S31 are shown in Figure 14. XRD analysis of sample S25, precipitated from 0.1 M $NH_4Fe(SO_4)_2$ solution at 90 °C for 21 days, indicated the presence of $NH_4Fe_3(OH)_6(SO_4)_2$ and α-FeOOH. Electron microphotograph of this sample confirmed the results of XRD. Big particles in micron range correspond to $NH_4Fe_3(OH)_6(SO_4)_2$ and small particles correspond to α-FeOOH. After aging of the solution 0.1 M $NH_4Fe(SO_4)_2$ + 0.1 M urotropin at 90 °C for 6 hours, the precipitate (sample S31) consisted of an amorphous fraction and α-FeOOH of very small crystallite size. Electron microphotograph of sample S31 shows amorphous-like aggregates and small α-FeOOH particles. For the highest concentrations used in the present work (0.5 M $NH_4Fe(SO_4)_2$ + 1 M urotropin) and after 21 days of aging of the precipitation system at 90 °C, very small α-FeOOH rods were obtained, as shown in Figure 15.

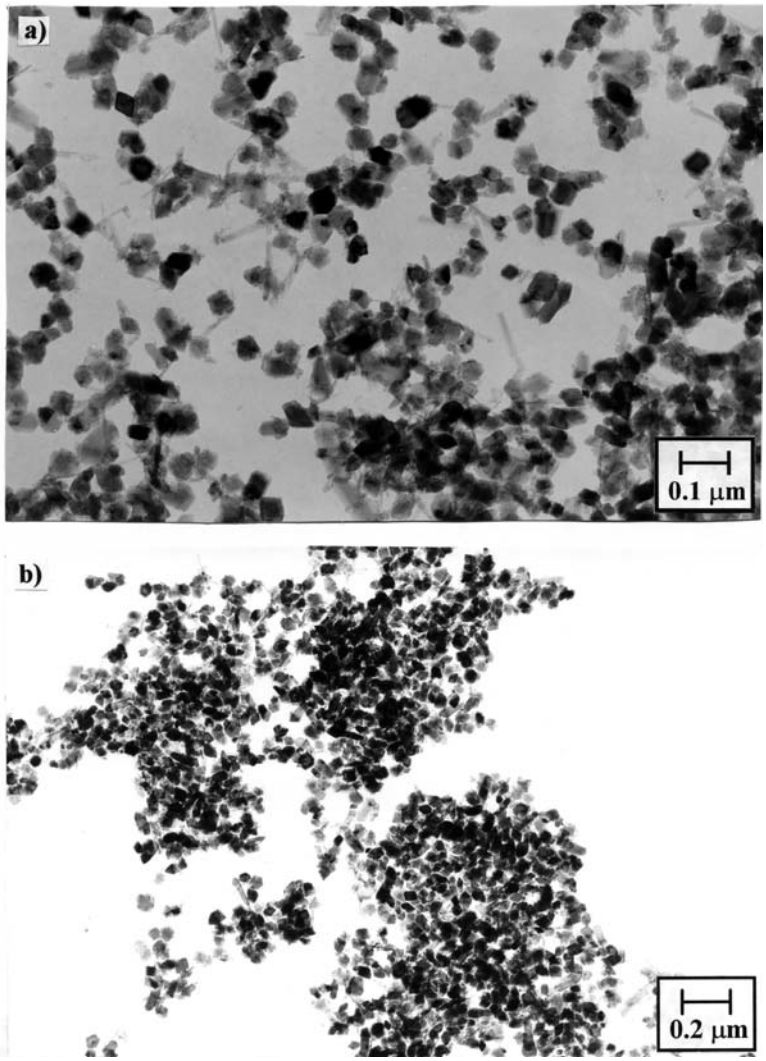

Figure 13. Transmisssion electron microphotographs of samples (a) S19 and (b) S20.

CONCLUSIONS

The effects of urotropin on the hydrolysis of Fe^{3+} ions in $NH_4Fe(SO_4)_2$ solutions at 90 °C were investigated. Urotropin was used as the generator of OH^- ions at working temperature. The precipitation systems were prepared in broad concentration regions, both for $NH_4Fe(SO_4)_2$ and urotropin, in order to obtain complete information about the overall precipitation process.

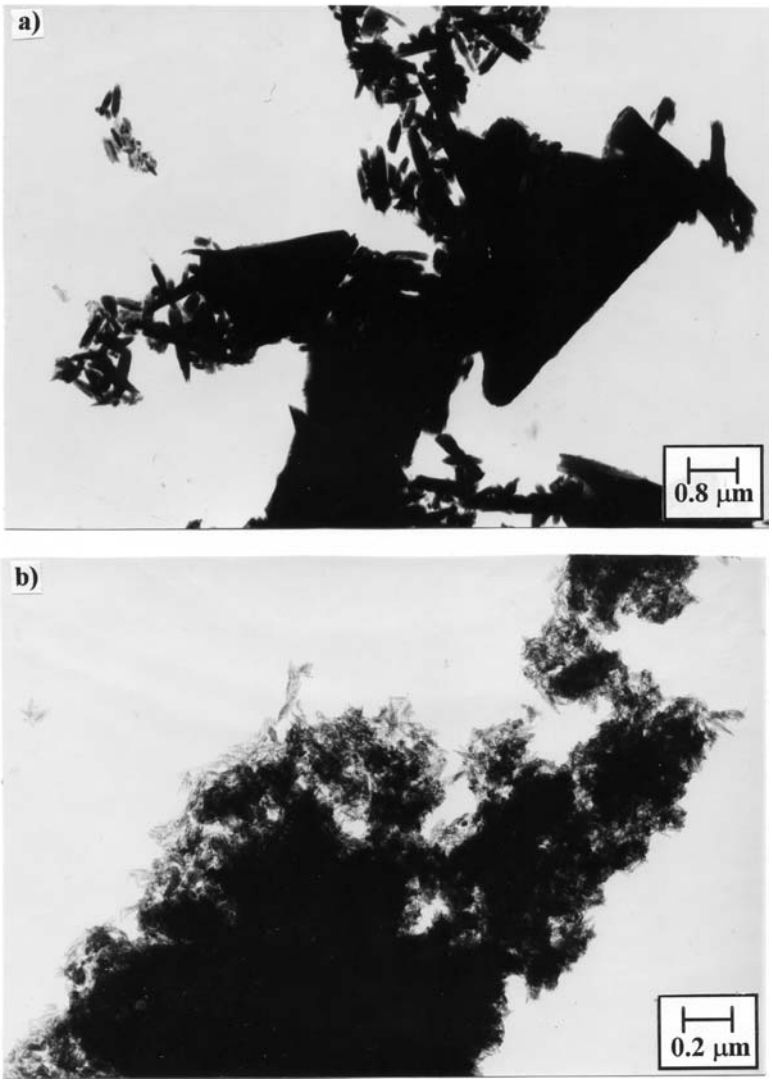

Figure 14. Transmisssion electron microphotographs of samples (a) S25 and (b) S31.

XRD, FT-IR and Mössbauer spectroscopies showed a very strong dependence of the chemical and structural properties of the precipitates on the concentrations of $NH_4Fe(SO_4)_2$ and urotropin, as well as on the time of hydrolysis. The amorphous character of precipitates was typical of the early stages of Fe^{3+} hydrolysis. In the precipitates, three crystalline phases were detected, α-FeOOH, α-Fe_2O_3 and $NH_4Fe_3(OH)_6(SO_4)_2$, and the specific

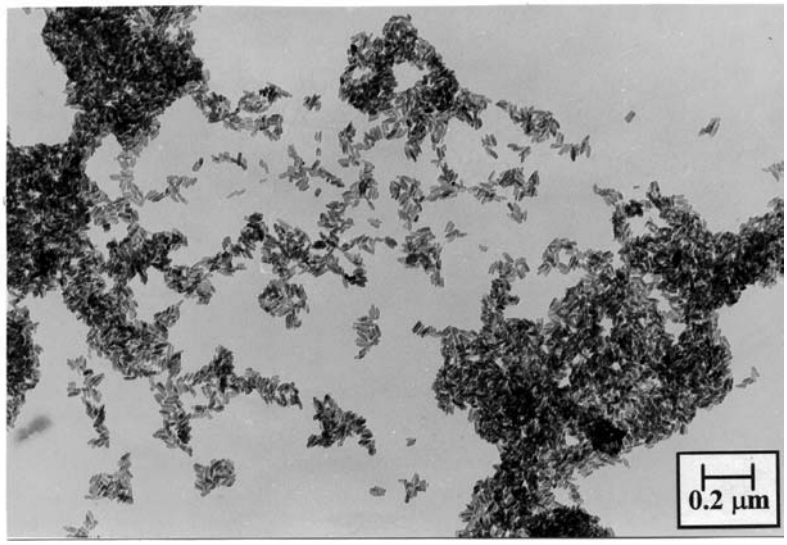

Figure 15. Transmisssion electron microphotograph of sample S62.

phase composition of each precipitate depended on the experimental conditions of its formation.

The present work also deals with the possible formation of schwertmannite in the early stages of forced hydrolysis of Fe^{3+} ions in the presence of sulphate anions. In several cases, FT-IR spectra similar to those of schwertmannite were recorded. In order to ascertain the possible presence of schwertmannite in the present samples, especially in those precipitated during short Fe^{3+} hydrolysis times, we compared literature data[21] of the XRD peak positions for jarosite, schwertmannite and goethite with the XRD patterns of our samples. The presence of schwertmannite was not confirmed in our samples. It is more probable that the amorphous fraction consisted of amorphous iron(III)-hydroxide particles containing significant amounts of sulphates on external as well as on internal surfaces due to the specific adsorption.

Regularity in the formation of solid phases by forced hydrolysis of $NH_4Fe(SO_4)_2$ solutions and the effect of urotropin were clearly visible. α-FeOOH precipitated from a 0.03 M $NH_4Fe(SO_4)_2$ solution, mixtures of $NH_4Fe_3(OH)_6(SO_4)_2$, and a small amount of α-FeOOH precipitated from 0.1 M $NH_4Fe(SO_4)_2$ solution, whereas $NH_4Fe_3(OH)_6(SO_4)_2$ precipitated as a single phase from 0.5 M $NH_4Fe(SO_4)_2$ solution. These results are in full accord with a previous work.[33] Mixtures of α-Fe_2O_3 and α-FeOOH precipitated from 0.03 M $NH_4Fe(SO_4)_2$ solutions containing 0.03 to 0.25 M urotropin.

The addition of 0.025 to 0.25 M urotropin to the 0.1 M $NH_4Fe(SO_4)_2$ solution suppressed the formation of $NH_4Fe_3(OH)_6(SO_4)_2$. α-FeOOH or mixtures of α-FeOOH and α-Fe_2O_3 were formed instead. On the other hand, in hydrolyzing a 0.5 M $NH_4Fe(SO_4)_2$ solution containing up to 0.25 M urotropin, $NH_4Fe_3(OH)_6(SO_4)_2$ was detected in the precipitates, whereas α-FeOOH precipitated for the concentration of urotropin ≥ 0.5 M. Mössbauer spectroscopy indicated that the α-FeOOH formed in these precipitation processes consisted of very fine (superparamagnetic) particles. Transmission electron microscopy showed formation of α-FeOOH particles of colloidal dimensions.

Acknowledgment. – We thank Professor Nikola Ljubešić for his assistance in transmission electron microscopic work.

REFERENCES

1. S. Musić, A. Vértes, G. W. Simmons, I. Czakó-Nagy, and H. Leidheiser, Jr., *J. Coll. Interface Sci.* **85** (1982) 256–266.
2. S. Musić, A. Vértes, G. W. Simmons, I. Czakó-Nagy, and H. Leidheiser, Jr., *J. Radiochem. Radioanal. Lett.* **49** (1981) 315–322.
3. R. S. Sapieszko, R. C. Patel, and E. Matijević, *J. Phys. Chem*. **81** (1977) 1061–1068.
4. T. Sugimoto, Y. Wang, H. Itoh, and A. Muramatsu, *Coll. Surfaces A: Physicochem. Eng. Aspects* **134** (1998) 265–279.
5. N. J. Reeves and S. Mann, *J. Chem. Soc., Faraday Trans*. **87** (1991) 3875–3880.
6. K. M. Parida and J. Das, *J. Mater. Sci*. **31** (1996) 2199–2205.
7. J. E. Dutrizac, *Hydrometallurgy* **42** (1996) 293–312.
8. S. Ozeki and K. Inouye, *J. Coll. Interface Sci*. **125** (1988) 356–358.
9. S. Musić, Z. Orehovec, S. Popović, and I. Czakó-Nagy, *J. Mater. Sci*. **29** (1994) 1991–1998.
10. N. Lazaroff, W. Sigal, and A. Wasserman, *Appl. Environ. Microbiol*. **43** (1982) 924–938.
11. K. Sasaki, M. Tsunekawa, T. Ohtsuka, and H. Konno, *Coll. Surfaces A: Physicochem. Eng. Aspects* **133** (1998) 269–278.
12. R. B. Herbert, Jr., *GFF (Geologiska Föreningens i Stockholm Förhandlingar*) **117** (1995) 81–85.
13. A. D. Karathanasis and Y. L. Thompson, *Soil Sci. Soc. Am. J*. **59** (1995) 1773–1781.
14. J. G. Webster, P. J. Swedlund, and K. S. Webster, *Environ. Sci. Technol*. **32** (1998) 1361–1368.
15. J. M. Bigham, U. Schwertmann, L. Carlson, and E. Murad, *Geochim. Cosmochim. Acta* **54** (1990) 2743–2758.
16. J. M. Bigham, U. Schwertmann, S. J. Traina, R. L. Winland, and M. Wolf, *Geochim. Cosmochim. Acta* **60** (1996) 2111–2121.
17. R. J. Barham, *J. Mater. Res.* **12** (1997) 2751–2758.
18. C. W. Childs, K. Inoue, and C. Mizota, *Chem. Geol*. **144** (1998) 81–86.
19. J. L. Bishop and E. Murad, *Schwertmannite on Mars? Spectroscopic analyses of schwertmannite , its relationship to other ferric minerals, and its possible presence in the surface material on Mars*, in: M. D. Dyar, C. McCammmon, and M. W.

Schaefer (Eds.), *Mineral Spectroscopy: A Tribute to Roger G. Burns,* The Geochemical Society, Special Publ. No 5, 1996, pp. 337–338.
20. Powder Diffraction File, International Centre for Diffraction Data, Newtown Square, Pa. 19073–3273, USA.
21. J. M. Bigham, U. Schwertmann, and G. Pfab, *Appl. Geochem*. **11** (1996) 845–849.
22. L. Verdonck, S. Hoste, F. F. Roelandt, and G. P. Van Der Kelen, *J. Molec. Struct.* **79** (1982) 273–279.
23. P. Cambier, *Clay Miner.* **21** (1986) 191–200.
24. C. Morterra, A. Chiorino, and E. Borello, *Mater. Chem. Phys*. **10** (1984) 119–138.
25. J. M. Bigham, L. Carlson, and E. Murad, *Mineral. Mag.* **58** (1994) 641–648.
26. C. J. Serna, C. Parada Cortina, and J. V. Garcia-Ramos, *Spectrochim. Acta* **42A** (1986) 729–734.
27. C. Parada Cortina, S. Lopez Andres, and O. Garcia Martinez, *An. Quim*. **79 B** (1983) 567–571.
28. M. Kamoun, A. Lautie, F. Romain, M. H. Limage, and A. Novak, *Spectrochim. Acta* **44A** (1988) 471–477.
29. S. Musić, M. Ristić, and M. Tonković, *Z. Wasser-Abwasser-Forsch* **19** (1986) 186–196.
30. S. Musić and M. Ristić, *J. Radioanal. Nucl. Chem*. **120** (1988) 289–304.
31. J. E. Iglesias and C. J. Serna, *Miner. Petrogr. Acta* **29A** (1985) 363–370.
32. Sh. Yariv and E. Mendelovici, *Appl. Spectr.* **33** (1979) 410–411.
33. S. Musić, S. Popović, and Z. Orehovec, *J. Coll. Interface Sci.* **160** (1993) 479–482.

SAŽETAK

Utjecaj urotropina na ubrzanu hidrolizu iona Fe^{3+} u otopinama $NH_4Fe(SO_4)_2$

Svetozar Musić, Ankica Šarić, Stanko Popović, Kiyoshi Nomura i Tsuguo Sawada

Utjecaj urotropina na hidrolizu iona Fe^{3+} u vodenim otopinama $NH_4Fe(SO_4)_2$ pri 90 °C istraživan je primjenom rentgenske difrakcije u prahu, Mössbauerove spektroskopije i FT-IR spektroskopije. U eksperimentima su korištene otopine $NH_4Fe(SO_4)_2$ (0.03, 0.1 i 0.5 mol dm^{-3}) koje su sadržavale i različite količine urotropina. Kemijska i strukturna svojstva taloga jako su ovisila o koncentracijama reaktanata i trajanju hidrolize. U početku hidrolize iona Fe^{3+} uzorci su bili pretežno amorfni. U talozima su nađene najviše tri kristalne faze: α-FeOOH, α-Fe_2O_3 i $NH_4Fe_3(OH)_6(SO_4)_2$, a fazni sastav taloga ovisio je o eksperimentalnim uvjetima. Faznom analizom taloga nije dokazano nastajanje švertmanita. Čestice amorfne frakcije taloga, ali i čestice α-FeOOH, sadržavale su znatne količine sulfata što je objašnjeno specifičnom adsorpcijom tog aniona. Nađena je zakonitost ovisnosti faznog sastava taloga o eksperimentalnim uvjetima. Veličine malih kristala nastalih oksidnih faza dobivene su na temelju proširenja difrakcijskih linija i primjenom Scherrerove jednadžbe. Superparamagnetsko ponašanje čestica α-FeOOH utvrđeno je Mössbauerovom spektroskopijom.